JOURNAL OF BACTERIOLOGY, Oct. 1994, p. 5988–5998
0021-9193/94/$04.00+0

Vol. 176, No. 19

MotX, the Channel Component of the Sodium-Type Flagellar Motor†

LINDA L. McCARTER*

Immunology Department, The Scripps Research Institute, La Jolla, California 92037

Received 17 May 1994/Accepted 25 July 1994

Thrust for propulsion of flagellated bacteria is generated by rotation of a propeller, the flagellum. The power to drive the polar flagellar rotary motor of *Vibrio parahaemolyticus* is derived from the transmembrane potential of sodium ions. Force is generated by the motor on coupling of the movement of ions across the membrane to rotation of the flagellum. A gene, *motX*, encoding one component of the torque generator has been cloned and sequenced. The deduced protein sequence is 212 amino acids in length. MotX was localized to the membrane and shown to interact with MotY, which is the presumed stationary component of the motor. Overproduction of MotX, but not that of a nonfunctional mutant MotX, was lethal to *Escherichia coli*. The rate of lysis caused by induction of *motX* was proportional to the sodium ion concentration. Li^+ and K^+ substituted for Na^+ to promote lysis, while Ca^{2+} did not enhance lysis. Protection from the lethal effects of induction of *motX* was afforded by the sodium channel blocker amiloride. The data suggest that MotX forms a sodium channel. The deduced protein sequence for MotX shows no homology to its ion-conducting counterpart in the proton-driven motor; however, in possessing only one hydrophobic domain, it resembles other channels formed by small proteins with single membrane-spanning domains.

Many bacteria swim by rotating semirigid helical propellers, or flagellar filaments, that are powered by rotary motors (9, 32, 54). The flagellar filament is attached via a flexible coupling to the core of the motor, the basal body. Surrounding the basal body, in the cytoplasmic membrane, are approximately 8 to 10 force-generating units (11, 26). Energy to drive the motor is not derived from ATP hydrolysis (29) but rather is from the transmembrane electrochemical potential of specific ions. Each torque-generating unit converts the electrochemical energy of the transmembrane potential to mechanical work. Somehow there is coupling of the flow of specific ions down a transmembrane potential gradient to rotation of the flagellum (24, 35, 42). For bacteria like *Escherichia coli* and *Bacillus subtilis*, the energy is supplied by the proton motive force, while for some alkaliphilic and marine bacteria, the energy is derived from the sodium motive force (25, 31). Thus, there are two types of flagellar motors, H^+ and Na^+ driven.

The proton-type torque generator of *E. coli* has been extensively studied. It is composed of two proteins, MotA and MotB. These proteins have been overproduced and localized to the cytoplasmic membrane (65). MotA contains four hydrophobic segments (16). A combination of genetic and biochemical evidence indicating that these segments probably are transmembrane domains and that MotA functions as a proton channel has accumulated (12, 13). Overproduction of a fusion protein containing MotA and part of the amino terminus of MotB suppresses growth, presumably because of proton leakage across the cytoplasmic membrane. Genetic studies have provided evidence for interaction between MotA and MotB (58). The studies of Chun and Parkinson (14) coupled with the deduced protein sequence (57) have allowed the development of a clear topological picture of MotB: it traverses the membrane once near its amino terminus, with the remainder of the protein localized in the periplasm. The protein is believed to serve the role of a linker, or stator, connecting the motor to a stationary component of the cell wall.

Until now, the sodium-type motor has not been described. The bacterium *Vibrio parahaemolyticus* possesses both proton- and sodium-type flagellar motors (4). It is a versatile organism, swimming in liquid environments by rotating a single polar flagellum and moving, or swarming, on solid surfaces and through viscous environments by using a second flagellar system with a different set of flagella, lateral flagella (38). These two types of flagella are powered by different energy sources. Two genes encoding components, LafT and LafU, of the proton-type force generator which drives the lateral flagella have been identified, cloned, and sequenced (41). Their deduced protein sequences resemble those of *E. coli* MotA and MotB, respectively. Recently, one component of the sodium-type motor, MotY, has been identified. Features of the deduced protein sequence suggest that MotY functions as a stator anchoring the force-generating unit to peptidoglycan, analogous in manner to MotB (39). This work characterizes a second component of the sodium-type motor, MotX. The data suggest that MotX functions as the sodium channel.

MATERIALS AND METHODS

Bacterial strains and growth conditions. The strains and plasmids used in this work are described in Table 1. The media for propagation of *V. parahaemolyticus* strains have been described previously (39). LB, 2× YT, and NZCYM media for propagation of *E. coli* strains and lambda were prepared as described by Sambrook et al. (49). LBK medium for propagation of sodium-sensitive strains was adapted from that described by Pinner et al. (46). LBK-K medium was LBK without KCl. Amiloride, chloramphenicol, and 5-bromo-4-chloro-3-indolyl phosphate (XP) were from Sigma Chemical Company. Chloramphenicol was used at a final concentration of 10 μg/ml, and XP was used at a final concentration of 40 μg/ml. A 225 mM stock solution of amiloride was prepared in dimethyl sulfoxide.

* Mailing address: Immunology Department IMM17-A, The Scripps Research Institute, 10666 North Torrey Pines Rd., La Jolla, CA 92037. Phone: (619) 554-4147. Fax: (619) 554-3786. Electronic mail address: mccarter@scripps.edu.

† Publication 8676-IMM from The Scripps Research Institute.

TABLE 1. Bacterial strains and plasmids

Strain or plasmid	Genotype or description	Source, parent, and/or reference
V. parahaemolyticus		
BB22	Wild type	7
LM1017	*lafX313*::*lux*	BB22; 37
LM4170	*lafX313*::*lux motX118*::mini-Mu *lac* (Tet^s)	37
LM4171	*lafX313*::*lux motY141*::mini-Mu *lac* (Tet^s)	37
LM4262	*motX1699*::Tn*phoA* (blue)	BB22; this work
LM4292	*lafX313*::*lux motX1726*::Tn*phoA* (blue)	LM1017; this work
LM4293	*lafX313*::*lux motX1727*::Tn*phoA* (light blue)	LM1017; this work
LM4286	*lafX313*::*lux hmp-1712*::Tn*phoA*	LM1017; this work
LM4291	*lafX313*::*lux hmp-1722*::Tn*phoA*	LM1017; this work
LM4287	*lafX313*::*lux purA1713*::Tn*phoA*	LM1017; this work
E. coli		
CC118	*araD139* Δ(*ara leu*)*7697* Δ*lacX74* Δ*phoA20 galE galK thi rpsE rpoB argE*(Am) *recA1*	22
DH5α	F$^-$ *endA1 hsdR17* (r_K^-) *supE44 thi-1* λ$^-$ *recA1 deoR gyrA96 relA1* Δ(*argF-lacZYA*)U169 φ80d*lacZ*ΔM15	Bethesda Research Laboratories
LLM1693	CC118/pLM1693	This work
LLM1758	DH5α/pLM1758	This work
LLM1766	DH5α/pLM1766	This work
LLM1784	DH5α/pLM1784	This work
LLM1785	DH5α/pLM1785	This work
Plasmids		
pKK388-1	Tet^r; Ap^r expression vector (P_{trc})	Clontech
pLAFRII	Tet^r; pLAFRI with polylinker	19
pMMB66EH	Ap^r expression vector (P_{tac}); ColE1 replicon; *lacI*^{q}	20
pUC18CMR	pUC18 with chloramphenicol resistance cassette	52
pLM1693	*motX*$^+$; pLAFRII recombinant cosmid complementing strain LM4170 for motility	*V. parahaemolyticus* bank; 40
pLM1699	*motX1699*::Tn*phoA*	pLM1693
pLM1737	3.3-kb *Pst*I fragment containing *motX1699*::Tn*phoA*, P_{trc} aligned	pKK388-1 and pLM1699
pLM1751	2.3-kb *Eco*RI fragment containing *motY* with P_{trc} promoter opposed	39
pLM1756	1.2-kb *Pst*I fragment containing *motX* with P_{tac} aligned	pLM1693 and pMMB66EH
pLM1758	Cam^r; 1.2-kb *Pst*I fragment containing *motX* with P_{tac} aligned	pLM1756 and pUC18CMR
pLM1766	Cam^r; pMMB66EH	pMMB66EH and pUC18CMR
pLM1784	pLM1758 (*motX*$^+$) plus 1.2-kb *Sph*I fragment containing *motY*, P_{tac} aligned with *motY* and *motX*	pLM1758 and pLM1751
pLM1785	pLM1766 plus 1.2-kb *Sph*I fragment containing *motY*, P_{tac} aligned with *motY*	pLM1766 and pLM1751

Genetic techniques. Mutagenesis with λTn*phoA* (from C. Manoil) (22) was performed by infecting a culture of *E. coli* LLM1693. This procedure and the procedures for conjugation and gene replacement in *V. parahaemolyticus* have been described elsewhere (51, 53). All strain constructions were confirmed by Southern blot analysis of restricted genomic DNA (36, 40) on 0.45-μm Magna Charge nylon membranes (Micron Separations Inc., Westborough, Mass.).

Plasmid constructions. Transformations, ligations, and other general procedures were adapted from the methods of Sambrook et al. (49). The 1.2-kb *Pst*I fragment encoding *motX* was cloned into the expression vector pMMB66EH to make pLM 1756. Plasmid pLM1756 was made into the chloramphenicol-resistant derivative pLM1758 by cloning the 1.6-kb *Bam*HI fragment containing a Cam^r cassette from pUC18CMR (52) into the *Bgl*II site following the *motX* gene. The *motY* gene was incorporated into pLM1758 by cloning a 1.2-kb *Sph*I fragment from pLM1751 into the *Sph*I site in the polylinker preceding *motX*. The isopropyl-β-D-thiogalactopyranoside (IPTG)-inducible promoter, P_{tac}, was aligned with *motY* and *motX*. A control plasmid, pLM1766, was constructed by introducing the Cam^r cassette into the *Bam*HI site in pMMB66EH. The 1.2-kb *Sph*I fragment containing *motY* was also cloned into pLM1766 to make pLM1785 (P_{tac} promoter aligned with *motY*). A 3.3-kb *Pst*I restriction fragment containing the fusion *motX1699*::Tn*phoA* was cloned into pKK388-1 to make pLM1737. The wild-type allele on the 1.2-kb *Pst*I fragment was also cloned into this vector; however, because induction of *motX* was lethal, it was preferable to work with the construct pLM1758, in which the *lacI* gene was incorporated directly into the clone and not carried separately on an F-prime plasmid.

Cell fractionation and SDS-PAGE. Cells were fractionated by using a variation of a method described previously for preparation of outer membrane samples (40); i.e., to obtain total membrane rather than outer membrane preparations, cells were lysed in one-half the original volume cold H_2O instead of 1% *N*-lauroyl sarkosine. Cytoplasmic fractions, which were the supernatants to the membrane pellets, were diluted 1:2 into 2× Laemmli sample buffer (LSB) (28), while whole cells and membrane samples were resuspended in 1 volume of 1× LSB. Protein samples were boiled for 5 min prior to separation by sodium dodecyl sulfate-polyacrylamide gel electrophoresis (SDS-PAGE) (2) and visualized by the method of Fairbanks et al. (17) for Coomassie blue staining (Brilliant Blue R; U.S. Biochemicals, Cleveland, Ohio). The resolving gels were 20 cm in length and were composed of 12.5% acrylamide. Acrylamide and SDS were from BDH (Poole, England), glycine was from GIBCO BRL (Gaithersburg, Md.), and the molecular weight markers (low-molecular-weight range) were from Bio-Rad Laboratories (Hercules, Calif.). Western blot (immunoblot) analysis has been described previously (41), and anti-alkaline phosphatase antiserum was from 5 Prime 3 Prime Inc. (Boulder Colo.).

DNA sequencing analysis. Sequences were determined by using a shotgun strategy, as follows. An 8.0-kb *Eco*RI fragment from pLM1693 was self-ligated and then sonicated to generate

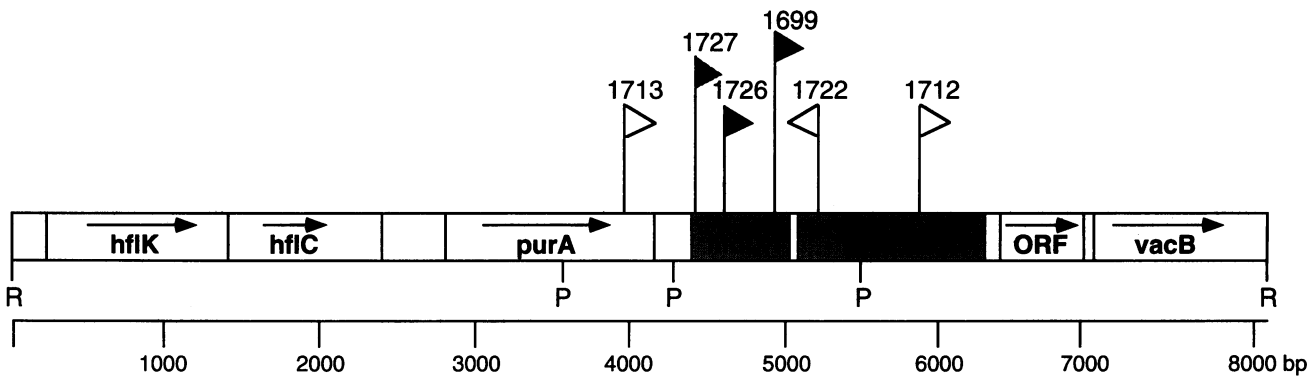

FIG. 1. Physical map of the *motX* locus. Restriction sites: R, *Eco*RI; P, *Pst*I. Tn*phoA* insertions are shown as flags on the restriction map. The tip of the flag points in the direction of transcription of *phoA*. Filled flags indicate transposons that confer a motility defect when introduced onto the chromosome of *V. parahaemolyticus*. The intensity of the fill represents the intensity of alkaline phosphatase color reaction on plates with a chromogenic substrate. Positions of the transposons were obtained by sequencing: 1713 is at bp 3938, 1727 is at bp 4440, 1726 is at bp 4623, 1699 is at bp 4980, 1722 is at bp 5213, and 1712 is at bp 5852. The locus is similar to the *E. coli hflK-purA* locus, and the ORFs are designated by the names of their homologs. Arrows indicate directions of transcription. The shaded regions (encoding *motX* and *hmp*) appear to be inserted into this locus. *E. coli hmp* encodes a hemoglobin-like protein (64). In the *E. coli purA* locus five ORFs have been sequenced (46, 66). Sequencing studies of an overlapping region in *S. flexneri* extended the fifth ORF, called *vacB* (63). The similarities, determined by Genetics Computer Group Bestfit analysis, of the deduced *V. parahaemolyticus* gene products are as follows: HflK, 71% similar and 57% identical to *E. coli* HflK; HflC, 73% similar and 55% identical to *E. coli* HflC; PurA, 88% similar and 77% identical to *E. coli* PurA; Hmp, 74% similar and 62% identical to *E. coli* Hmp; ORF, 76% similar and 63% identical to *E. coli* ORF and 80% similar and 66% identical to *S. flexneri* ORF; and VacB, 78% similar and 66% identical to *E. coli* VacB and 78% similar and 64% identical to *S. flexneri* VacB. The exact positions of the ORFs are as follows: 225..1427, 1430..2410, 2854..4170, 4400..5035, complement (5118..6302), 6461..6886, and 7002..>8150.

random subfragments 300 to 600 bp in length (5). After end repair with T4 DNA polymerase, the subfragments were ligated into the *Sma*I site of M13mp8 (43) and sequenced by the dideoxy-chain termination procedure of Sanger et al. (50) with the Sequenase 2.0 kit from U.S. Biochemicals. The source of radioactivity was α^{35}-S-dATP (Amersham). Nucleotide sequence was obtained for both strands. Synthetic oligonucleotides, prepared by Integrated DNA Technologies, Inc. (Coralville, Iowa), were occasionally used as primers on long templates to obtain additional sequence. Sequence assembly was performed by using Roger Staden's sequence assembly program (SAP; version 5.0) (56), and the Genetics Computer Group software package version 7.0 was used for sequence analysis. Searches for homology were performed at the National Center for Biotechnology Information with the BLAST network service (1). Tn*phoA* insertions in plasmid pLM1693 were sequenced directly by using oligonucleotide primers specific to each unique end of Tn*phoA* (primer L, 5′ CAGA GCGGCAGTCTGATCAC 3′, and primer R, 5′ CCGCAC GATGAAGAGCAG 3′).

Nucleotide sequence accession number. The entire nucleotide sequence of 8,152 bases shown in Fig. 1 has been assigned GenBank accession number U09005.

RESULTS

Cloning of the *motX* locus. Screening of a collection of mini-Mu transposon mutants defective in swimming motility identified two strains with defects, *mot-118* and *mot-141*, potentially in the polar flagellar motor (37). These strains were unable to move in semisolid motility agar or when viewed in wet mounts in the light microscope. Inspection of electron micrographs showed that these bacteria possessed single polar flagella that were indistinguishable from the polar flagella of the wild type. Thus, these strains produced flagella that seemed paralyzed. Complementation of the motility defects in strains LM4170 (*mot-118*) and LM4171 (*mot-141*) allowed the retrieval of clones from a cosmid bank of *V. parahaemolyticus* DNA. Two families of cosmids were obtained: one that restored swimming motility to strain LM4170 and one that restored motility to LM4171. Therefore, the mutations were in two unlinked genes, *motX* and *motY*, required for rotation of the polar flagellum. A representative cosmid, pLM1693, of the class complementing the *motX118* defect was chosen for further analysis.

***motX* maps alone.** Cosmid pLM1693 contained greater than 20 kb of recombinant *V. parahaemolyticus* DNA. When this cosmid was used to probe Southern blots of restricted chromosomal DNAs prepared from the wild type and LM4170, an 8-kb *Eco*RI fragment was perturbed in the mutant strain but not in the wild type. The *motX* gene was further localized by using the transposon Tn*phoA*. Transposon insertions that mapped in the 8-kb *Eco*RI fragment were isolated on the cosmid (Fig. 1). Tn*phoA* can be used as a probe for transported proteins (34). The transposons in blue clones (i.e., those that formed active, transported fusions on indicator plates with a chromogenic substrate) mapped to a 1.2-kb *Pst*I restriction fragment. All of the blue transposons yielded swimming motility-defective phenotypes when introduced into the *V. parahaemolyticus* chromosome. Gene disruption with the remaining transposons, which mapped in the 8-kb fragment and flanked the 1.2-kb *Pst*I fragment, had no effect on swimming motility.

Transposon mutagenesis suggested and DNA sequencing of the 8-kb *Eco*RI restriction fragment confirmed that *motX* mapped alone, in the absence of other flagellar genes. The gene appears to be interposed at the equivalent of 95 min on the *E. coli* chromosome in the *purA* locus (Fig. 1). In *E. coli* five open reading frames (ORFs) have been sequenced at that locus (45). Sequencing studies of an overlapping region in *Shigella flexneri* extended the fifth ORF, called *vacB* (63). Sequencing of the *V. parahaemolyticus motX* locus revealed homologs to these same five ORFs. The gene encoding MotX appears to be inserted into this region, as does one other gene, *hmp*, which codes for a potential hemoglobin-like protein (64).

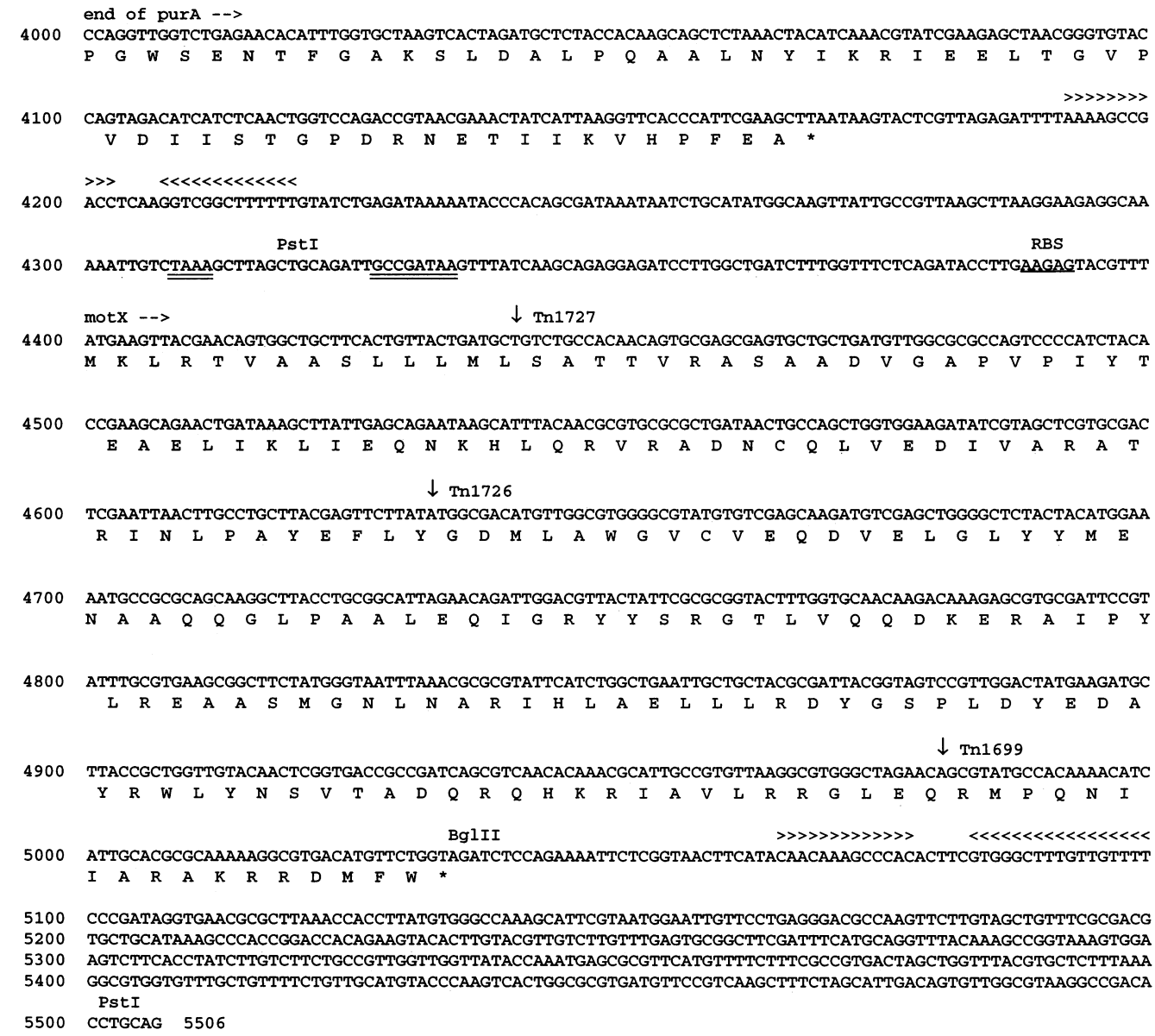

FIG. 2. DNA nucleotide and deduced amino acid sequences of *motX*. Selected restriction sites are shown to facilitate orientation to the physical map. The features of a potential σ^{28} promoter are double underlined. A site resembling the Shine-Dalgarno sequence of the *E. coli* ribosome binding site (RBS) is underlined. Chevrons indicate structures that could serve as transcriptional terminators. Arrows indicate the points of insertion of transposons, which are designated by their specific numbers.

DNA nucleotide sequence and predicted amino acid sequence. The DNA sequence corresponding to bp 4000 to 5506 on the map in Fig. 1 is presented in Fig. 2 along with the deduced amino acid sequence for MotX. The ORF starts with an ATG codon that is preceded by features resembling those of an *E. coli* ribosome binding site. Upstream of *motX* are sequences that match the consensus derived for σ^{28} flagellar promoters: $TAAAN_{15}GCCGATAA$ (N_{15} represents 15 nucleotides) (23). Downstream of *motX* are sequences that resemble an *E. coli* rho-independent terminator. Disruption of this ORF by transposons 1727, 1726, and 1699 resulted in motility-defective phenotypes when the transposons were transferred to the chromosome. The exact point of insertion of each transposon is shown in Fig. 2 and was determined by DNA sequencing from the ends of each transposon. The insertion of these three transposons resulted in the formation of fusion proteins with alkaline phosphatase. This enzyme is not active unless it is transported out of the cytoplasm, i.e., to the cytoplasmic membrane or beyond. Strains carrying clones with transposons 1726 and 1699 exhibited high levels of alkaline phosphatase activity, indicated by a deep blue color on plates with a chromogenic substrate, whereas a strain with transposon 1727 was lighter blue. The *motX* gene encodes a potential polypeptide 212 amino acids in length. It contains one potential membrane-spanning domain, composed of 27 predominantly hydrophobic amino acids, located near the amino terminus. Both transposons 1699 and 1726 map to the carboxyl-terminal side of the hydrophobic domain. The fusion joint created by

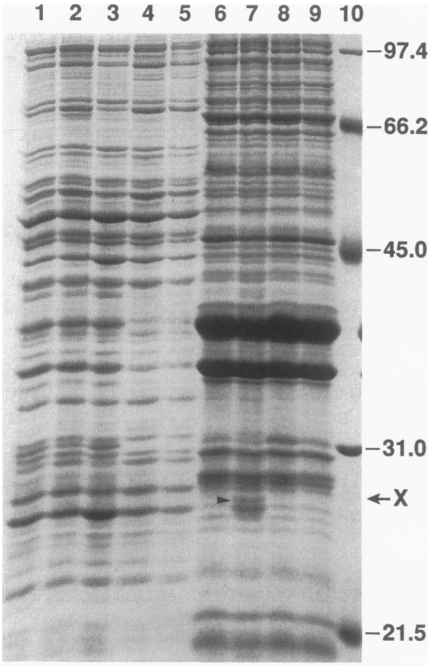

FIG. 3. Identification and localization of MotX. An exponentially growing culture of a strain with plasmid pLM1758, which contains *motX* under the control of an IPTG-inducible promoter, was diluted into fresh LBK-K medium (plus chloramphenicol) with and without 2 mM IPTG. Samples were harvested by centrifugation 100 min postinduction. The control strain, LLM1766, harbored the vector without an insert. Samples were resuspended directly into LSB (whole cells [WC]) or were fractionated into cytoplasmic (C) and total membrane (M) fractions. Proteins were visualized on SDS-PAGE stained with Coomassie blue. Lanes: 1, LLM1758 without IPTG (WC); 2, LLM1758 with IPTG (WC); 3, LLM1766 with IPTG (WC); 4, LLM1758 without IPTG (C); 5, LLM1758 with IPTG (C); 6, LLM1758 without IPTG (M); 7, LLM1758 with IPTG (M); 8, LLM1766 without IPTG (M); 9, LLM1766 with IPTG (M); and 10, molecular weight standards. Membrane samples were loaded with samples concentrated approximately fivefold compared with whole-cell and cytoplasmic preparations. MotX is indicated by the arrow and arrowhead, and the sizes of the molecular weight standards are given in thousands on the right.

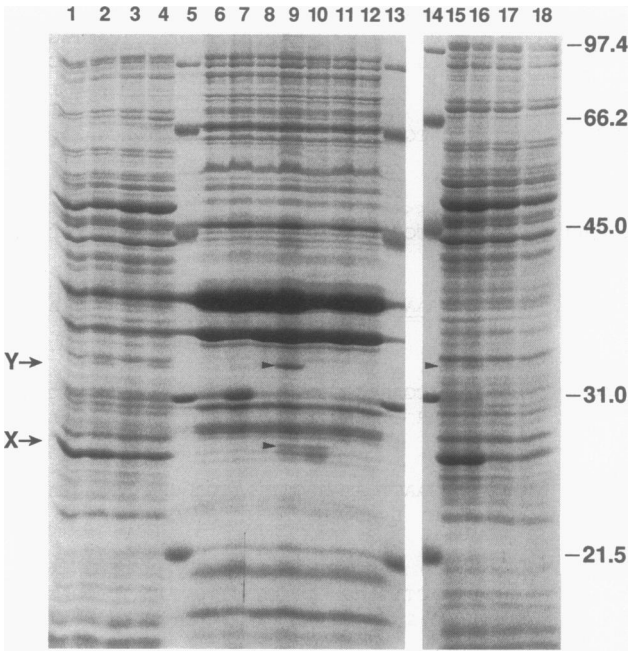

FIG. 4. Localization of MotY coproduced with MotX. Exponentially growing cultures of strains with pLM1784 (*motY*$^+$ *motX*$^+$), pLM1785 (*motY*$^+$), pLM1758 (*motX*$^+$), and pLM1766 (vector alone) were diluted into fresh LBK-K medium (plus chloramphenicol) with and without 2 mM IPTG, and the samples were harvested by centrifugation 100 min postinduction. Samples were resuspended directly into LSB (whole cells [WC]) or were fractionated into cytoplasmic (C) and membrane (M) fractions. Lanes: 1, LLM1785 without IPTG (WC); 2, LLM1785 with IPTG (WC); 3, LLM1784 without IPTG (WC); 4, LLM1784 with IPTG (WC); 5, molecular weight standards; 6, LLM1785 without IPTG (M); 7, LLM1784 without IPTG (M); 8, LLM1785 with IPTG (M); 9, LLM1784 with IPTG (M); 10, LLM1758 with IPTG (M); 11, LLM1758 without IPTG (M); 12, LLM1766 with IPTG (M); 13 and 14, molecular weight standards; 15, LLM1785 without IPTG (C); 16, LLM1785 with IPTG (C); 17, LLM1784 without IPTG (C); and 18, LLM1784 with IPTG (C). Membrane samples were loaded with samples concentrated approximately fivefold compared with whole-cell and cytoplasmic preparations. MotX and MotY are indicated by arrows and arrowheads, and the sizes of the molecular weight standards are given in thousands on the right.

transposon 1727 occurs at the ninth amino acid in the hydrophobic domain. When the deduced sequence for MotX was used to search data banks, the protein appeared to be novel. No significant similarities were found.

Identification and localization of MotX. The 1.2-kb *Pst*I fragment containing *motX* was subcloned into the expression vector pMMB66EH, which has the IPTG-inducible P_{tac} promoter and carries its own repressor gene, *lacI*^{q}. Exponentially growing cultures of strains LLM1758 and LLM1766 (carrying the control plasmid with no insert) were diluted into fresh medium with and without 2 mM IPTG. Optical density was measured to monitor growth rate, and samples were periodically harvested for fractionation and analysis on protein gels. No new protein bands were seen when whole-cell profiles of strain LLM1758 grown with the inducer were compared with those of the same strain grown without the inducer (Fig. 3, lanes 2 and 1, respectively) or with those of an induced culture of control strain LLM1766 (lane 3). Proteins in the cytoplasmic fractions harvested from LLM1758 grown with or without inducer also looked similar (Fig. 3, lanes 5 and 4, respectively); however, there was a new protein synthesized that is visible in the membrane fraction harvested from the induced culture (lane 7) but that was not present in the uninduced membrane fraction (lane 6) or in the uninduced and induced membrane fractions from the control strain (lanes 8 and 9, respectively). This protein migrated with an apparent molecular mass of 28 kDa (the predicted molecular mass is 24.1 kDa).

Interaction of MotX and MotY. Previously, the gene product of *motY* was identified as a protein with an apparent molecular mass of 33 kDa on SDS-PAGE. In order to compare and investigate the functions of MotX and MotY, the genes encoding these proteins were cloned separately and together under the control of the P_{tac} promoter in the vector pMMB66EH. Plasmid pLM1785 contains *motY*, and plasmid pLM1784 contains *motY* and *motX*. Induction of strain LLM1785 and LLM1784 with IPTG led to production of a 33-kDa protein that can be seen in whole-cell profiles on SDS-PAGE (Fig. 4, lanes 1 through 4). Membrane samples prepared from induced strain LLM1785 (lane 8) resembled the preparations from uninduced strains LLM1785 and LLM1784 and from the induced control strain LLM1766 (lanes 6, 7, and

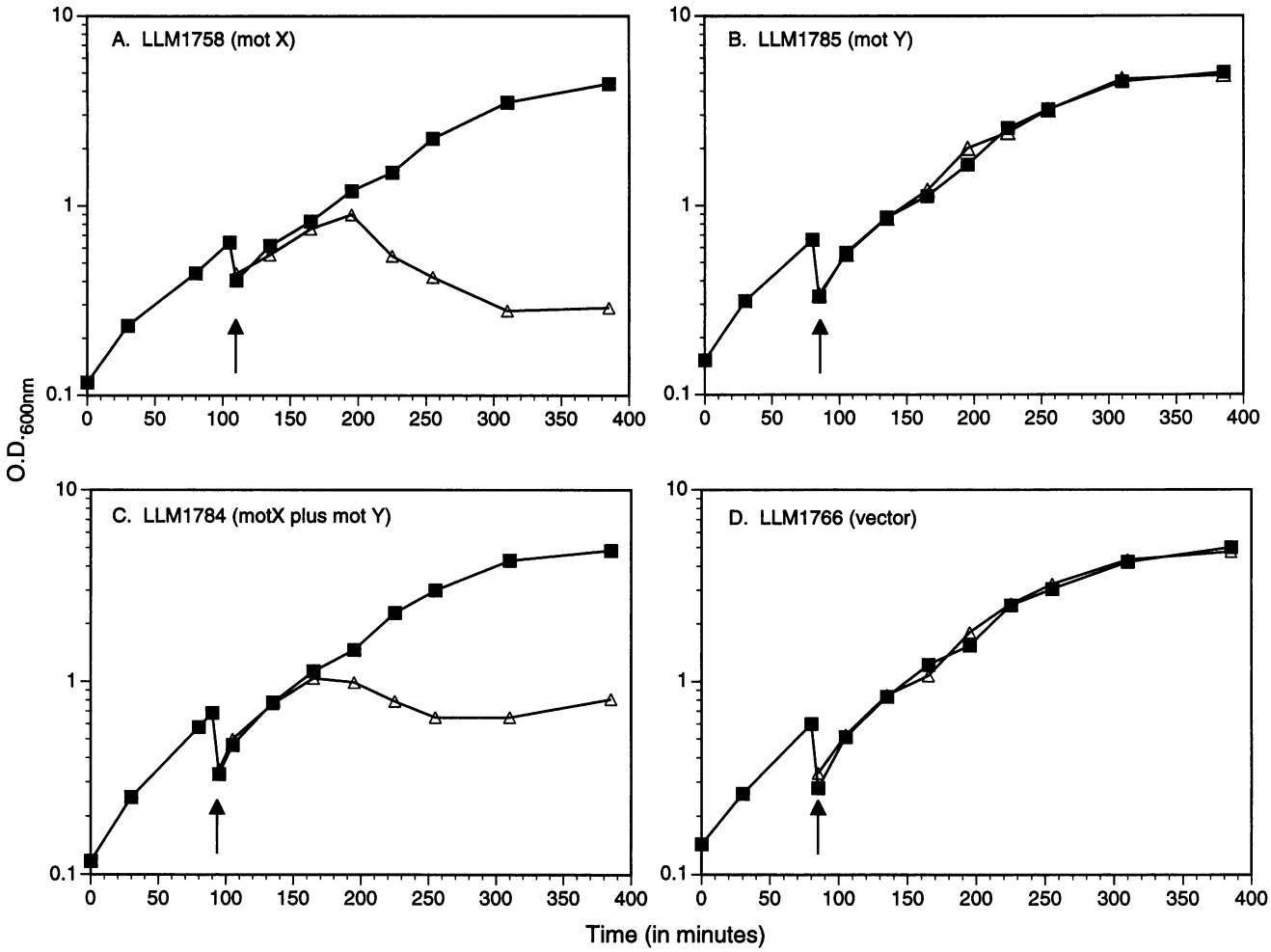

FIG. 5. Induction of *motX* kills the cell. Strains containing plasmids with *motX* and/or *motY* under the control of an IPTG-inducible promoter were grown in 2× YT medium plus chloramphenicol with aeration to mid-exponential phase, at which time (indicated by arrows) the cultures were diluted into 2× YT–chloramphenicol medium supplemented (triangles) or not supplemented (squares) with 2 mM IPTG. Growth of the cultures was monitored by measuring the optical density at 600 nm ($O.D._{600nm}$).

12, respectively). Unlike MotX (lane 10), MotY failed to localize to the membrane fraction of strain LLM1785 and could be detected in the cytoplasmic fraction (uninduced versus induced; lanes 15 and 16, respectively). However, its cellular location was changed when MotY was coproduced with MotX on induction of strain LLM1784. MotY was not observed in the cytoplasmic fraction (uninduced versus induced; lanes 17 and 18, respectively), but rather both MotX and MotY were found in the membrane fraction of induced LLM1784 (lane 9). When the membranes were extracted with *N*-lauroyl sarkosine, which selectively solubilizes inner membrane proteins, MotX and MotY disappeared from the preparations (data not shown). Thus, MotY localizes to the cytoplasmic membrane in the presence of MotX.

Overproduction of MotX, but not MotY, kills the cell. When exponentially growing cultures of LLM1758 (*motX*$^+$) or LLM 1784 (*motX*$^+$ *motY*$^+$) were diluted into fresh medium and induced with IPTG, induction of Mot protein synthesis was deleterious to cell growth. As shown in Fig. 5A and C, when growth was monitored by measuring the optical density at 600 nm, cultures continued to grow postinduction for approximately 1.5 doubling times, at which point the rate of exponential growth began to decline, and after a certain point cell lysis became apparent. This was not true for strains with *motY* alone (LLM1785; Fig. 5B) or with the control plasmid (LLM1766; Fig. 5D). Induction did not affect growth of the cultures. Thus, induction of *motX*, but not induction of *motY*, was lethal to the cell.

The killing resulting from induction of *motX* seemed to be specific for the function of the induced protein rather than a nonspecific effect of overproduction of a membrane protein. A *Pst*I fragment containing the MotX-alkaline phosphatase fusion created by transposon 1699 was subcloned into an expression vector. Fusion 1699 was exported, as indicated both by a deep blue color on plates with a chromogenic alkaline phosphatase substrate and by localization experiments using antiserum directed against alkaline phosphatase to detect the fusion protein in Western blots. The fusion product was not functional, since transposon 1699 caused a motility defect when it was introduced into the *V. parahaemolyticus* chromosome. Overproduction of the fusion protein, which is functionally inactive but which localizes to the membrane, did not affect the growth curve: induced and uninduced cultures were indis-

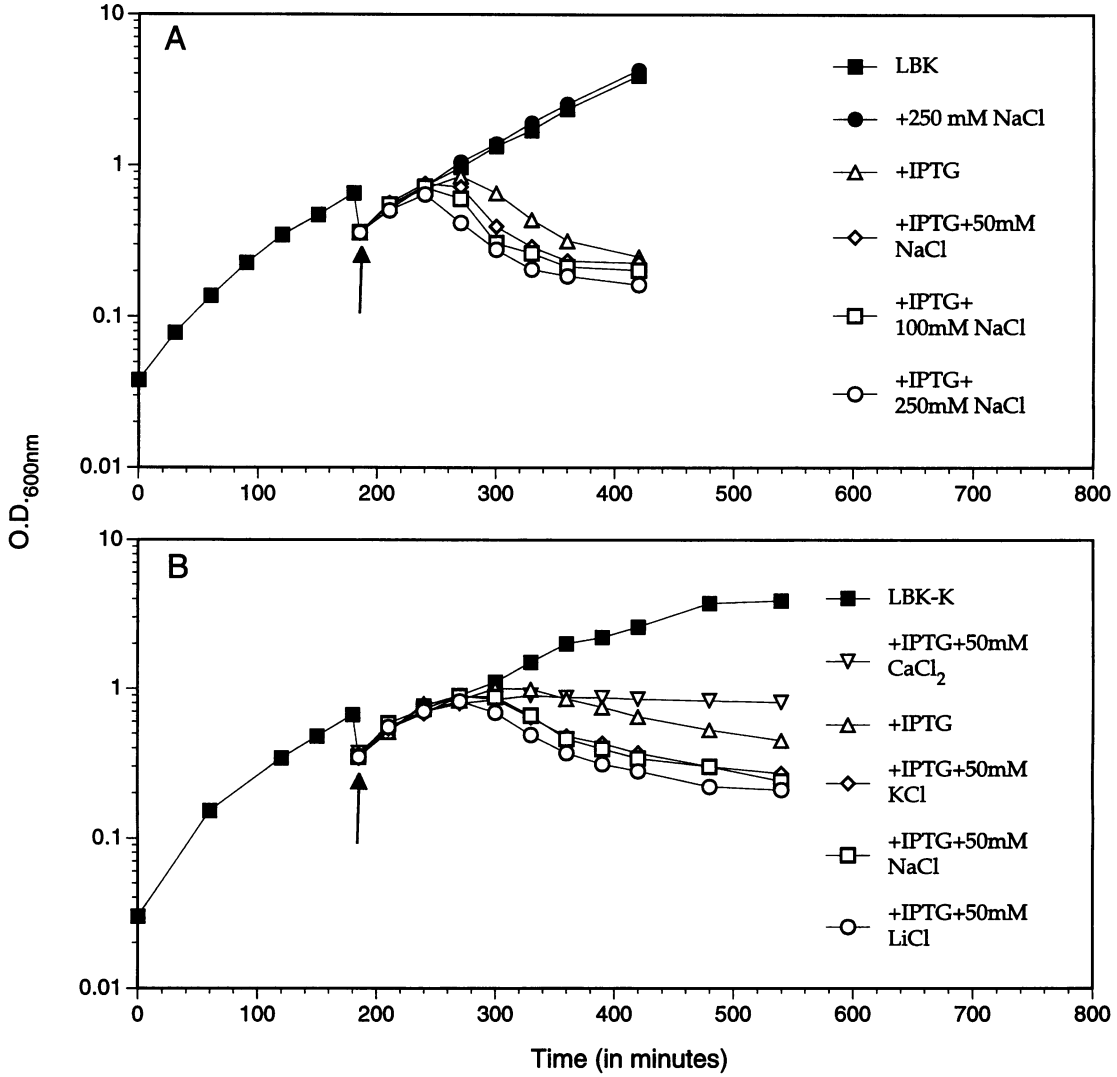

FIG. 6. (A) Effect of NaCl on postinduction growth. Strain LLM1758, which contains *motX* under the control of an IPTG-inducible promoter, was diluted into LBK (LB medium with KCl substituted for NaCl) plus chloramphenicol and grown with aeration to mid-exponential phase, at which time (indicated by arrows) the culture was diluted into LBK-chloramphenicol medium supplemented as indicated with inducer and various concentrations of NaCl. IPTG, when added, was at a final concentration of 2 mM. Growth of the cultures was monitored by measuring the optical density at 600 nm ($O.D._{600nm}$). (B) Effect of other ions on postinduction growth. The experimental design was similar to that for panel A except that LLM1758 was grown in LBK medium without KCl (LBK-K). Supplements were as indicated.

tinguishable from each other and from cultures with the vector alone.

Evidence that MotX forms an ion channel. To investigate the nature of the growth inhibition and cell lysis resulting from overproduction of MotX, the effect of sodium ion concentration on postinduction growth was examined by using a medium appropriate for sodium-sensitive strains, i.e., L broth in which the sodium was replaced by KCl (LBK; 46). Medium with no added sodium ions was most permissive for growth in the presence of inducer (Fig. 6A). The postinduction rate of decrease in optical density was enhanced by an increased concentration of NaCl in the medium. Increasing concentrations of sodium ions led to increasing rates of decline in the optical density at 600 nm.

Cell death could also be promoted by the addition of lithium ions to the induction medium (Fig. 6B). As was the case for Na^+, the rate of decline in postinduction optical density was proportional to the concentration of Li^+ (data not shown). Cells were able to grow in LBK medium without supplementation with KCl (LBK-K). This allowed examination of the effect of K^+ on growth. As can be seen in Fig. 6B, addition of K^+ to the postinduction medium promoted a decline in the optical density of the culture. In contrast, addition of $CaCl_2$ to the induction medium did not increase the rate of lysis and in fact provided some protection. $CaCl_2$ did not affect the level of induction of *motX*: the protein product could be found in membrane fractions prepared from cells grown with inducer in the presence of $CaCl_2$.

The drug amiloride is a known inhibitor of sodium channels in animal cells and is a specific inhibitor of Na^+-driven flagellar motors (60). When amiloride was added to the medium in induction experiments similar to those described above, there was some protection against the deleterious effects of induction of *motX*. The rate of lysis was diminished by increasing

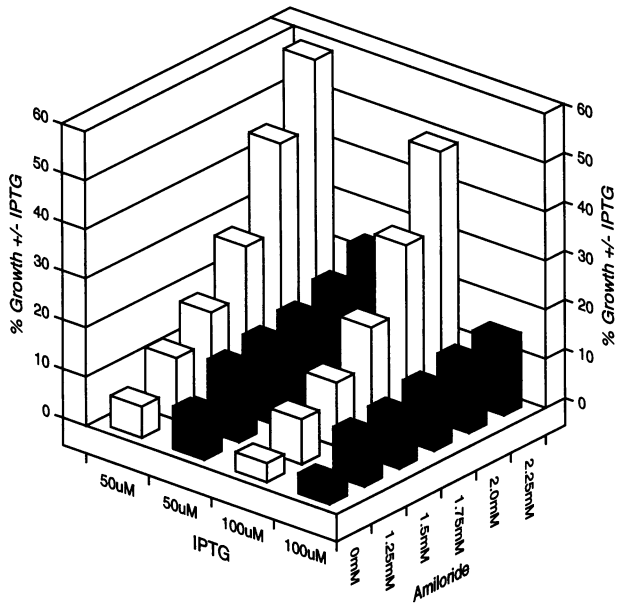

FIG. 7. Amiloride protection. Strain LLM1758, which contains *motX* under the control of an IPTG-inducible promoter, was diluted into fresh LBK medium plus chloramphenicol and grown with aeration to mid-exponential phase, at which time the culture was diluted into LBK-chloramphenicol medium supplemented as indicated (open bars, no NaCl added; solid bars, 250 mM NaCl added). Cultures were grown for 5.5 h postdilution, and the optical density at 600 nm was measured. Results are expressed as the percent ratio of the final optical density achieved with inducer added to that without inducer in a particular concentration of amiloride. The effect of amiloride was examined at two concentrations of inducer, 50 and 100 μM IPTG. The values are the averages from two experiments. The highest concentration of amiloride (2.25 mM) approaches the limits of amiloride solubility in growth medium.

amiloride concentrations. Cells continued to grow, albeit very slowly, in the presence of inducer plus amiloride. The results presented in Fig. 7 are expressed as percent growth, or the ratio of the optical density of a culture grown in a particular amiloride concentration with IPTG to the optical density of the culture grown in the same medium without IPTG measured 5.5 h postinduction; thus, they are essentially survival rates. Increasing concentrations of amiloride gave increasing survival rates. The amount of protection afforded by amiloride was a function of the degree of induction of MotX. Less protection by equivalent concentrations of amiloride was seen at higher concentrations of inducer (e.g., 100 versus 50 μM). At even higher concentrations of inducer (1 mM), no protection was seen (data not shown). The protective effect of amiloride was antagonized in the presence of NaCl. Approximately the same, low levels of survival were attained at all concentrations of amiloride when 250 mM NaCl was added to the medium. It is known that amiloride inhibits rotation of the polar flagellum in a competitive manner with sodium ions.

DISCUSSION

To swim, some bacteria use a flagellar propeller and a reversible, rotary motor. Electrochemical energy stored as membrane potential is converted to mechanical energy used to rotate the propeller. Some types of motors use the proton motive force, while others use the sodium motive force. The mechanism of energy conversion is still a mystery, although the components of proton-type motors have been well studied. Characterization of the sodium-driven torque generator of the polar flagellum of *V. parahaemolyticus* has just begun. In addition to chemomechanical coupling, other transducing events occur at this flagellum. The polar flagellum is thought to also function as a dynamometer (37). The bacterium senses a flagellum unable to rotate, perhaps by detecting a stalled motor. By sensing forces that restrict movement of the flagellum, the bacterium detects physical aspects of its environment, namely, a surface or highly viscous layer. This physical information is somehow transduced to reprogram gene expression, directing differentiation to a new cell type, the swarmer cell, that is adapted for growth on and colonization of surfaces. Thus, for a number of reasons, it is of interest to gain more information about the polar, sodium-type flagellar motor of *V. parahaemolyticus*.

A multitude of genes are involved in flagellar motility, and flagellar genes are generally found organized in large clusters (33). Moreover, motor genes previously characterized are organized in operons. In *E. coli* and *B. subtilis*, the *mot* operons are linked to chemotaxis genes (3, 44, 55, 67). In *V. parahaemolyticus*, the lateral flagellar (proton-type) motor genes are linked and are in an operon with the lateral flagellar sigma gene and some other flagellar genes (41). Two genes encoding components of the polar flagellar (sodium-type) motor have been identified, and they appear to be novel with respect to operon organization, genetic linkage, and gene structure. The genes encoding MotX and MotY are not in an operon. They do not map together, and they do not map near other flagellar components. MotY appears to be inserted into a locus similar to the *E. coli rnt* locus, and MotX appears to be inserted into the equivalent of the *E. coli purA* locus. Finally, nucleotide and deduced protein sequences do not resemble those of known motility or flagellar genes.

For the proton-type motor of *E. coli*, two cytoplasmic membrane proteins, MotA and MotB, are required for torque generation. MotA is the proton conductor (12). It possesses four potential membrane-spanning domains believed to be important for proton movement (16). Dominant, nonfunctional mutations map to all four of these hydrophobic regions (13). Although the physical nature of the interaction has not been elucidated, the coupling between the passage of ions and flagellar rotation appears to be very tight (10, 42). The role of MotB is postulated to be one of a stator, linking MotA to some stationary component, such as the cell wall (14). Such a configuration would enable the torque generator to remain stationary when force is applied to the filament base; however, there is no evidence for what component MotB is specifically anchored to. MotY seems to fulfill the stator function for the sodium-type flagellar motor, and the data suggest that it interacts directly with peptidoglycan (39). Although it shows no sequence similarity to MotB, it does possess, like MotB, a single potential membrane-spanning domain. In addition, it has a carboxyl-terminal domain that shows striking similarity to those of a number of proteins known to interact with peptidoglycan, e.g., OmpA and peptidoglycan-associated lipoprotein. This domain is not readily recognizable in *E. coli*. In this report a second component, MotX, required for sodium-type motor function is characterized. The gene was cloned and sequenced. The deduced product is a small, 212-amino-acid polypeptide with a single potential membrane-spanning domain. The protein was localized to the cytoplasmic membrane. Tn*phoA* fusions mapping distal to this domain exhibited alkaline phosphatase activity. On overproduction of MotX, a new

protein that migrated at 28 kDa appeared in membrane preparations.

The dramatic result of overproduction of MotX in *E. coli* was cell death. This damaging effect was specific to the function of the protein rather than due to general effects on growth caused by overproduction of a membrane protein. Overproduction of a nonfunctional fusion protein had no detrimental effect on growth. MotX alone was sufficient to cause severe growth impairment; MotY coproduction was not required. The results suggest that MotX forms the sodium-conducting component of the torque generator. Cells induced for the production of MotX became sensitive to the NaCl concentration of the growth medium. Increasing concentrations of NaCl lead to faster rates of cell death on induction of MotX. The sodium channel blocker amiloride (6, 8) provided protection to the cell on induction of MotX. When the drug amiloride, which is a known competitive inhibitor of the sodium-type flagellar motor (24), was present in the inducing medium, lysis was prevented and the cells continued to slowly grow. The protection was concentration dependent and could be titrated by the amount of MotX produced. Furthermore, protection by amiloride was removed in the presence of 250 mM NaCl. Specificity for monovalent ions could be demonstrated. In addition to Na^+, Li^+ and K^+ were effective at promoting lysis on induction, while Ca^{2+} was not. By measuring the swimming motility of the closely related bacterium *Vibrio alginolyticus*, Liu and colleagues (30) found that lithium but not potassium could substitute for sodium, whereas Imae and Atsumi (24) reported that lithium could not substitute for sodium for alkaliphilic *Bacillus* species. It will be interesting to study the ion-conducting properties of the sodium-type motor for *V. parahaemolyticus*. Perhaps specificity is simply organism dependent or, more interestingly, ion translocation and torque generation can be separable events. It also seems possible that ion selectivity is conferred by additional components of the motor.

There is precedent for the existence of channels formed by small polypeptides with single membrane-spanning domains. A voltage-gated potassium channel found in mammals is generated by a protein 130 amino acids in length (Ut1 or MinK) (18, 21, 48, 59, 62), and a proton-conducting channel of the influenza virus is formed by M2, which is 97 amino acids in length (47). M2, like both MotX and MotY, contains two cysteine residues, and the pore of M2 is formed by a homotetramer composed of two disulfide-linked dimers (61). M2, MinK, and MotX possess single hydrophobic domains bounded on each side by charged moieties. In this respect they resemble the bacterial pore-forming colicins (15). The minimum length of an active peptide fragment of colicin E1 is 88 residues; however, unlike that of M2, the colicin pore is formed by a single molecule.

MotX and MotY look more like each other than they look like other proteins (Fig. 8). Data bank searches for homology revealed significant matches with only the carboxyl-terminal region of MotY, which seems to contain a domain important for peptidoglycan interaction. Both molecules have a stretch of predominantly hydrophobic residues at their amino termini that are of sufficient length to be membrane spanning and are bounded on either side by charged residues. Approximately equidistant from the amino terminus of each molecule is the identical tetrapeptide CQLV, and both molecules have a second cysteine residue. MotX and MotY interact. MotY, when produced in *E. coli*, localized to the membrane only when it was coproduced with MotX and not when it was produced by itself. The hydrophobicity of the putative membrane-spanning domain as determined from a Kyte-Doolittle hydropathy plot

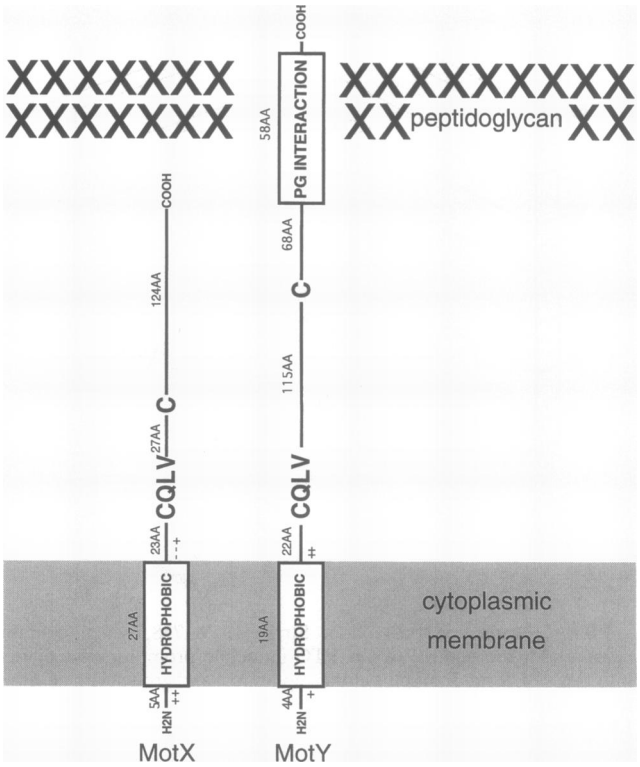

FIG. 8. Comparison of MotX and MotY. Both MotX and MotY possess single hydrophobic domains of sufficient length to span a membrane. The MotX domain has the greater hydrophobic character. The potential transmembrane domains are bounded on each side by charged amino acids, indicated by + or −. MotX localizes to the cytoplasmic membrane, and Tn*phoA* fusions that map to the carboxyl side of the hydrophobic domain are active. Interaction of MotY with MotX may direct or stabilize insertion of MotY in the membrane, for MotY localizes to the membrane only in the presence of MotX. At its carboxyl terminus MotY possesses a domain that may be important for interaction with peptidoglycan (PG). Note that each molecule has two cysteine residues and a homologous tetrapeptide equidistant from the hydrophobic domains. The GenBank accession number for MotX is U09005, and that for MotY is U06949.

(27) is considerably greater for MotX than for MotY. MotX may direct or stabilize MotY in the cytoplasmic membrane. This laboratory hopes to probe the interactions between these proteins and to determine the architecture of the force generator, as well as to gain insight as to the nature of the sodium channel itself. It should be possible to identify the amiloride interaction site. How Na^+ is conducted through the membrane and whether MotX forms an open pore-like channel or is more like a carrier/porter protein will be of much interest.

ACKNOWLEDGMENTS

I thank Deborah Noack for her outstanding technical assistance, Austin Kwon and Paul Moe for isolation of Tn*phoA* insertions, Howard Berg and Phil Matsumura for critical review of the manuscript, and Brian Tack for helpful discussions.

This research was supported by Public Health Service grant GM43196 from the National Institutes of Health.

REFERENCES

1. **Altschul, S. F., W. Miller, E. W. Myers, and D. J. Lipman.** 1990. Basic local alignment search tool. J. Mol. Biol. **215**:403–410.
2. **Ames, G. F.-L.** 1974. Resolution of bacterial proteins by polyacryl-

amide gel electrophoresis on slabs. J. Biol. Chem. **249**:634–644.
3. **Armstrong, J. B., and J. Adler.** 1969. Location of genes for motility and chemotaxis on the *Escherichia coli* genetic map. J. Bacteriol. **97**:156–161.
4. **Atsumi, T., L. McCarter, and Y. Imae.** 1992. Polar and lateral flagellar motors of marine *Vibrio* are driven by different ion membrane forces. Nature (London) **355**:182–184.
5. **Bankier, A. T., and B. G. Barrell.** 1983. Shotgun DNA sequencing, p. 1–34. *In* R. A. Flavell (ed.), Techniques in nucleic acid biochemistry. Elsevier/North-Holland Scientific, Limerick, Ireland.
6. **Barbry, P., O. Chassande, D. Duval, B. Rousseau, C. Frelin, and M. Lazdunski.** 1989. Biochemical identification of two types of phenamil binding sites associated with amiloride-sensitive Na^+ channels. Biochemistry **28**:3744–3749.
7. **Belas, R., M. Simon, and M. Silverman.** 1986. Regulation of lateral flagella gene transcription in *Vibrio parahaemolyticus*. J. Bacteriol. **167**:210–218.
8. **Benos, D. J., S. Cunningham, R. R. Baker, K. B. Beason, Y. Oh, and P. R. Smith.** 1992. Molecular characteristics of amiloride-sensitive sodium channels. Rev. Physiol. Biochem. Pharmacol. **120**:32–63.
9. **Berg, H. C., and R. A. Anderson.** 1973. Bacteria swim by rotating their flagellar filaments. Nature (London) **245**:380–382.
10. **Berg, H. C., and L. Turner.** 1993. Torque generated by the flagellar motor of *Escherichia coli*. Biophys. J. **65**:2201–2216.
11. **Blair, D. F., and H. C. Berg.** 1988. Restoration of torque in defective flagellar motors. Science **242**:1678–1681.
12. **Blair, D., and H. C. Berg.** 1990. The MotA protein of *E. coli* is a proton-conducting component of the flagellar motor. Cell **60**:439–449.
13. **Blair, D. F., and H. C. Berg.** 1991. Mutations in the MotA protein of *Escherichia coli* reveal domains critical for proton conduction. J. Mol. Biol. **221**:1433–1442.
14. **Chun, S. Y., and J. S. Parkinson.** 1988. Bacterial motility: membrane topology of the *Escherichia coli* MotB protein. Science **230**:276–277.
15. **Cramer, W. A., F. S. Cohen, A. R. Merrill, and H. Y. Song.** 1990. Structure and dynamics of the colicin E1 channel. Mol. Microbiol. **4**:519–526.
16. **Dean, G. E., R. M. Macnab, J. Stader, P. Matsumura, and C. Burks.** 1984. Gene sequence and predicted amino acid sequence of the *motA* protein, a membrane-associated protein required for flagellar rotation in *Escherichia coli*. J. Bacteriol. **159**:991–999.
17. **Fairbanks, G., T. L. Steck, and D. F. H. Wallace.** 1971. Electrophoretic analysis of the major polypeptides of the human erythrocyte membrane. Biochemistry **10**:2606–2617.
18. **Folander, K., J. S. Smith, J. Antanavage, C. Bennett, R. B. Stein, and R. Swanson.** 1990. Cloning and expression of the delayed-rectifier IsK channel from neonatal rat heart and diethylstilbestrol-primed rat uterus. Proc. Natl. Acad. Sci. USA **87**:2975–2979.
19. **Friedman, A., S. R. Long, S. E. Brown, W. J. Buikema, and F. Ausubel.** 1982. Construction of a broad host range cosmid cloning vector and its use in the genetic analysis of *Rhizobium* mutants. Gene **18**:289–296.
20. **Fuerste, J. P., W. Pansegrau, R. Frank, H. Blocker, P. Scholz, M. Bagdasarian, and E. Lanka.** 1986. Molecular cloning of the plasmid RP4 primase region in a multi-host-range *tacP* expression vector. Gene **48**:119–131.
21. **Goldstein, S. A. N., and C. Miller.** 1991. Site-specific mutations in a minimal voltage-dependent K^+ channel alter ion selectivity and open-channel block. Neuron **7**:403–408.
22. **Gutierrez, C., J. Barondess, C. Manoil, and J. Beckwith.** 1987. The use of transposon Tn*phoA* to detect genes for cell envelope proteins subject to a common regulatory stimulus. J. Mol. Biol. **195**:289–297.
23. **Helmann, J. D.** 1991. Alternative sigma factors and the regulation of flagellar gene expression. Mol. Microbiol. **5**:2875–2882.
24. **Imae, Y., and T. Atsumi.** 1989. Na^+ driven bacterial flagellar motors. J. Bioenerg. Biomembr. **21**:705–716.
25. **Imae, Y., H. Matsukura, and S. Kobayashi.** 1986. Sodium-driven flagellar motors of alkalophilic *Bacillus*. Methods Enzymol. **125**: 582–592.
26. **Khan, S., and M. Dapice.** 1988. Effects of *mot* gene expression on the structure of the flagellar motor. J. Mol. Biol. **202**:575–584.
27. **Kyte, J., and R. F. Doolittle.** 1982. A simple method for displaying the hydropathic character of a protein. J. Mol. Biol. **157**:105–132.
28. **Laemmli, U. K.** 1970. Cleavage of structural protein during the assembly of the head of bacteriophage T4. Nature (London) **227**:680–685.
29. **Larsen, S. H., J. Adler, J. J. Gargus, and R. W. Hogg.** 1974. Chemomechanical coupling without ATP: the source of energy for motility and chemotaxis in bacteria. Proc. Natl. Acad. Sci. USA **71**:1239–1243.
30. **Liu, J. Z., M. Dapice, and S. Khan.** 1990. Ion selectivity of the *Vibrio alginolyticus* flagellar motor. J. Bacteriol. **172**:5236–5244.
31. **Macnab, R. M.** 1986. Proton-driven bacterial flagellar motor. Methods Enzymol. **125**:563–579.
32. **Macnab, R. M.** 1987. Flagella, p. 70–83. *In* F. C. Neidhardt, J. L. Ingraham, K. B. Low, B. Magasanik, M. Schaechter, and H. E. Umbarger (ed.), *Escherichia coli* and *Salmonella typhimurium* cellular and molecular biology. ASM Press, Washington, D.C.
33. **Macnab, R. M., and J. S. Parkinson.** 1991. Genetic analysis of the bacterial flagellum. Trends Genet. **7**:196–200.
34. **Manoil, C., and J. Beckwith.** 1985. Tn*phoA*: a transposon probe for protein export signals. Proc. Natl. Acad. Sci. USA **82**:8129–8133.
35. **Manson, M. D., P. Tedesco, H. C. Berg, F. M. Harold, and C. V. D. Drift.** 1977. A protonmotive force drives bacterial flagella. Proc. Natl. Acad. Sci. USA **74**:3060–3064.
36. **Martin, M., R. Showalter, and M. Silverman.** 1989. Identification of a locus controlling expression of luminescence genes in *Vibrio harveyi*. J. Bacteriol. **171**:2406–2414.
37. **McCarter, L., M. Hilmen, and M. Silverman.** 1988. Flagellar dynamometer controls swarmer cell differentiation of *V. parahaemolyticus*. Cell **54**:345–351.
38. **McCarter, L., and M. Silverman.** 1990. Surface-induced swarmer cell differentiation of *Vibrio parahaemolyticus*. Mol. Microbiol. **4**:1057–1062.
39. **McCarter, L. L.** 1994. MotY, a component of the sodium-type flagellar motor. J. Bacteriol. **176**:4219–4225.
40. **McCarter, L. L., and M. Silverman.** 1987. Phosphate regulation of gene expression in *Vibrio parahaemolyticus*. J. Bacteriol. **169**:3441–3449.
41. **McCarter, L. L., and M. E. Wright.** 1993. Identification of genes encoding components of the swarmer cell flagellar motor and propeller and a sigma factor controlling differentiation of *Vibrio parahaemolyticus*. J. Bacteriol. **175**:3361–3371.
42. **Meister, M., G. Lowe, and H. C. Berg.** 1987. The proton flux through the bacterial flagellar motor. Cell **49**:643–650.
43. **Messing, J.** 1983. New M13 vectors for cloning. Methods Enzymol. **101**:20–78.
44. **Mirel, D. B., V. M. Lustre, and M. J. Chamberlin.** 1992. An operon of *Bacillus subtilis* motility genes transcribed by the σ^D form of RNA polymerase. J. Bacteriol. **174**:4197–4204.
45. **Noble, J. A., M. A. Innis, E. V. Koonin, K. E. Rudd, F. Banuett, and I. Herskowitz.** 1993. The *Escherichia coli hflA* locus encodes a putative GTP-binding protein and two membrane proteins, one of which contains a protease-like domain. Proc. Natl. Acad. Sci. USA **90**:10866–10870.
46. **Pinner, E., Y. Kotler, E. Padan, and S. Schuldiner.** 1993. Physiological role of NhaB, a specific Na^+/H^+ antiporter in *Escherichia coli*. J. Biol. Chem. **268**:1729–1734.
47. **Pinto, L. H., L. J. Holsinger, and R. A. Lamb.** 1992. Influenza virus M2 protein has ion channel activity. Cell **69**:517–528.
48. **Pragnell, M., K. J. Snay, J. S. Trimmer, N. J. MacLusky, F. Naftolin, L. K. Kaczmarek, and M. B. Boyle.** 1990. Estrogen induction of a small, putative K^+ channel mRNA in rat uterus. Neuron **4**:807–812.
49. **Sambrook, J., E. F. Fritsch, and T. Maniatis.** 1989. Molecular cloning: a laboratory manual, 2nd ed. Cold Spring Harbor Laboratory, Cold Spring Harbor, N.Y.
50. **Sanger, F., S. Nicklen, and A. R. Coulson.** 1977. DNA sequencing with chain-terminating inhibitors. Proc. Natl. Acad. Sci. USA **74**:5463–5467.
51. **Sar, N., L. McCarter, M. Simon, and M. Silverman.** 1989. Chemotactic control of the two flagellar systems of *Vibrio parahaemo-*

lyticus. J. Bacteriol. **172**:334–341.
52. **Schweizer, H. P.** 1990. The pUC18CM plasmids: a chloramphenicol resistance gene cassette for site-directed insertion and deletion mutagenesis in *Escherichia coli*. Biotechniques **8**:612–616.
53. **Silverman, M., R. Showalter, and L. McCarter.** 1991. Genetic analysis in *Vibrio*. Methods Enzymol. **204**:515–536.
54. **Silverman, M., and M. Simon.** 1974. Flagellar rotation and the mechanism of bacterial motility. Nature (London) **249**:73–74.
55. **Silverman, M., and M. Simon.** 1976. Operon controlling motility and chemotaxis in *E. coli*. Nature (London) **264**:577–580.
56. **Staden, R.** 1984. Computer methods to locate signals in nucleic acid sequences. Nucleic Acids Res. **12**:505–519.
57. **Stader, J., P. Matsumura, D. Vacante, G. E. Dean, and R. M. Macnab.** 1986. Nucleotide sequence of the *Escherichia coli motB* gene and site-limited incorporation of its product into the cytoplasmic membrane. J. Bacteriol. **166**:244–252.
58. **Stolz, B., and H. C. Berg.** 1991. Evidence for interactions between MotA and MotB, torque-generating elements of the flagellar motor of *Escherichia coli*. J. Bacteriol. **173**:7033–7037.
59. **Sugimoto, T., Y. Tanabe, R. Shigemoto, M. Iwai, T. Takumi, H. Ohkubo, and S. Nakanishi.** 1990. Immunohistochemical study of a rat membrane protein which induces a selective potassium permeation: its localization in the apical membrane portion of epithelial cells. J. Membr. Biol. **113**:39–47.
60. **Sugiyama, S., J. E. J. Cragoe, and Y. Imae.** 1988. Amiloride, a specific inhibitor for the Na^+-driven flagellar motors of alkalophilic *Bacillus*. J. Biol. Chem. **263**:8215–8219.
61. **Sugrue, R. J., and A. J. Hay.** 1991. Structural characteristics of the M2 protein of influenza A viruses: evidence that it forms a tetrameric channel. Virology **180**:617–624.
62. **Takumi, T., H. Ohkubo, and S. Nakanishi.** 1988. Cloning of a membrane protein that induces a slow voltage-gated potassium current. Science **242**:1042–1045.
63. **Tobe, T., C. Sasakawa, N. Okada, Y. Honma, and M. Yoshikawa.** 1992. *vacB*, a novel chromosomal gene required for expression of virulence genes on the large plasmid of *Shigella flexneri*. J. Bacteriol. **174**:6359–6367.
64. **Vasudevan, S. G., W. L. F. Armarego, D. C. Shaw, P. E. Lilley, N. E. Dixon, and R. K. Poole.** 1991. Isolation and nucleotide sequences of the *hmp* gene that encodes a haemoglobin-like protein in *Escherichia coli* K-12. Mol. Gen. Genet. **226**:49–58.
65. **Wilson, M. L., and R. M. Macnab.** 1990. Cooverproduction and localization of the *Escherichia coli* motility proteins MotA and MotB. J. Bacteriol. **172**:3932–3939.
66. **Wolfe, S. A., and J. M. Smith.** 1988. Nucleotide sequence and analysis of the *purA* gene encoding adenylosuccinate synthetase of *Escherichia coli* K12. J. Biol. Chem. **263**:19147–19153.
67. **Zuberi, A. R., C. Ying, H. M. Parker, and G. W. Ordal.** 1990. Transposon Tn*917lacZ* mutagenesis of *Bacillus subtilis*: identification of two new loci required for motility and chemotaxis. J. Bacteriol. **172**:6841–6848.